Memoirs of the School of Engineering, Okayama University, Vol. 18, No. 1, January 1984

Optical Circuit for Waveform-synthesis with Utilizing both GaAs- and Si-Optoelectronic Switches

Hiroya SANO*, Ryuji KOGA*, Megumi KOSAKA*, and Ichiro WAKE*

(Received December 27, 1983)

SYNOPSIS

This paper presents an optical-waveform synthesizer as one of the applications of optical bistable devices. This device is advantageous in terms of faster operation in which width of each pulse obtained is down to the order of subnanosecond, because this device employs both GaAs- and Si-optoelectronic switches as photodetector. Optical pulse shaping as a preliminary experiment is also described.

1. INTRODUCTION

Devices for optical signal processing have received much attention and advanced a lot recently.(1) On the future aspect of their applications, however, it is too early to make definite remarks. Among those devices, optical bistable devices have been greatly investigated and are expected to be one of the most important elements to realize an optical computer. For, as one of the applications of these devices, optical multivibrators or optical pulse generators can be constructed. Optical bistable devices (OBD's) are roughly classified into two groups by the type of feedback. One is all-optical or "intrinsic" type of OBD's, and the other, "hybrid" type. Intrinsic devices generally employ a Fabry-Perot resonator containing a nonlinear medium inside, and optical feedback is given to the medium. Hybrid ones are based on the principle that electric signals proportional to optical ones are fed back to an electrooptic crystal which shows nonlinear refraction. In both cases, some kind of feedback is necessary for optical bistability. Hybrid OBD's can be applied as optical functioning devices to optoelectronic systems where optical signals co-operate with electric ones. Intrinsic devices have the advantage in fabricating systems dealing with pure-optical signals. And by using small sized semiconductor-intrinsic devices, ultra-fast switching elements are expected possible.(2)

---

* Department of Electronics

In this paper, we present high-speed-hybrid devices which work as optical-waveform synthesizer. Further applications are open to compose optical multivibrators. These devices employ GaAs- and Si-optoelectronic switches as photodetector, that gives the devices faster operation compared with conventional hybrid devices with photodiodes as detector. As a preliminary experiment, we performed optical-pulse shaping by using optical pulses from a dye laser (pulse width ≈3ns) as a light source and Si OE switches only without GaAs ones.

2. OPTICAL-WAVEFORM SYNTHESIZER

2.1 Device Schematic and Principle

Figure 1 shows a schematic of the waveform synthesizer introduced in Chap. 1. This device employs two electrooptic modulators which are controlled by a Si optoelectronic (OE) switch and a GaAs OE switch, respectively. The modulator controlled by the Si OE switch, called MOD.1, produces a step-wise optical pulse $P_{in}(t)$ with a rise-time on the order of picosecond and a pulse width of approximately 100 nanosecond because a carrier lifetime in Si is on the same order.(3) The optical pulse $P_{in}(t)$ is incident on the modulator controlled

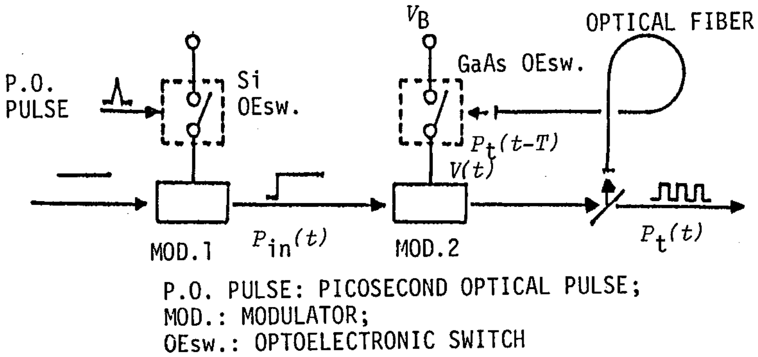

Fig. 1 Optical-Waveform Synthesizer with GaAs- and Si-Optoelectronic Switches.

by the GaAs OE switch, MOD.2. The GaAs OE switch is triggered by the transmitted optical pulse $P_t(t-T)$ delayed by the optical fiber. Suppose that at time $t=0$, a picosecond optical pulse triggers the Si OE switch. Then, $P_{in}(t)$ can be written as

$$P_{in}(t) = P\, U(t) \tag{1}$$

where $U(t)$ denotes a unit step function. In time interval $0<t<T$, MOD.2 is in a transparent state owing to an off-state of the GaAs OE switch, and $P_t(t)$ is in the "high" state. At $t=T$, $P_t(t-T)$ triggers the GaAs OE switch, that makes the MOD.2 opaque, and $P_t(t)$ falls into the

"low" state. That means at $t=2T$, $P_t(t-T)$ transits to the "low" state, and the GaAs OE switch follows on account of the shorter carrier lifetime in GaAs (≈100ps[4]). Hence, $P_t(t)$ comes up to the "high" state again, and those switching actions go on. Therefore, the transmitted optical power $P_t(t)$ is roughly represented by the expression

$$P_t(t) = P\ [U(t) - U(t-T) + U(t-2T) - U(t-3T) + U(t-4T) - \ldots\ ] \quad (2)$$

which is synthesized of the incident optical power.

2.2 "Auston"-Type Optoelectronic Switches

Since optoelectronic switches are basic elements to construct the optical-waveform synthesizer, this section mentions optoelectronic switches. As shown in Fig. 2, OE switches are in the microstripped transmission-line configuration. These switches were first investigated much by Auston.[5] So OE switches in Fig. 2 are sometimes called "Auston"-type OE switches. OE switches can generate a high-power electric pulse with a rise-time of less than 10 ps[5] on being triggered by a picosecond optical pulse. Therefore, these switches are very useful for the systems where ultra-fast switching is required such as measuring systems for picosecond optical pulses.

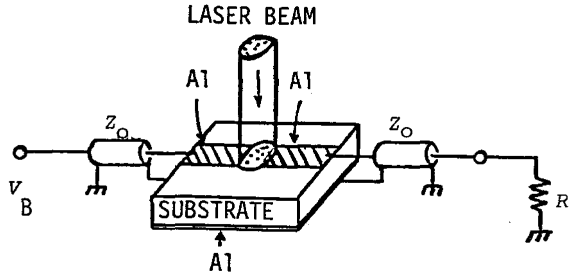

Fig. 2 "Auston"-Type Si Optoelectronic Switch.

In Fig. 2, on the top of the Si substrate, two Al electrodes are evaporated, and they are opposite across a small gap. The back plane is uniformly evaporared with Al to make the ground plane. When the gap is irradiated with an intense-visible-laser pulse, that causes photoconductivity near the surface of the substrate, giving ultra-fast switching. The schematic for GaAs OE switch is the same as one in Fig. 2, and switching speed is also on the same order.[6] However, fall-off characteristics of Si switches are much slower than those of GaAs ones by the reason of the difference of the carrier lifetimes.

Figure 3 indicates the oscillograms of the response of Si OE switch triggered by light from a dye laser (eastimated pulse width ≈3ns) pumped by the N_2 laser. In those oscillograms, the rise-time is limited by the bandwidth of the oscilloscope used (100MHz). The practical rise-time can be evaluated as less than 330 ps from the experiment mentioned in Chap. 3.

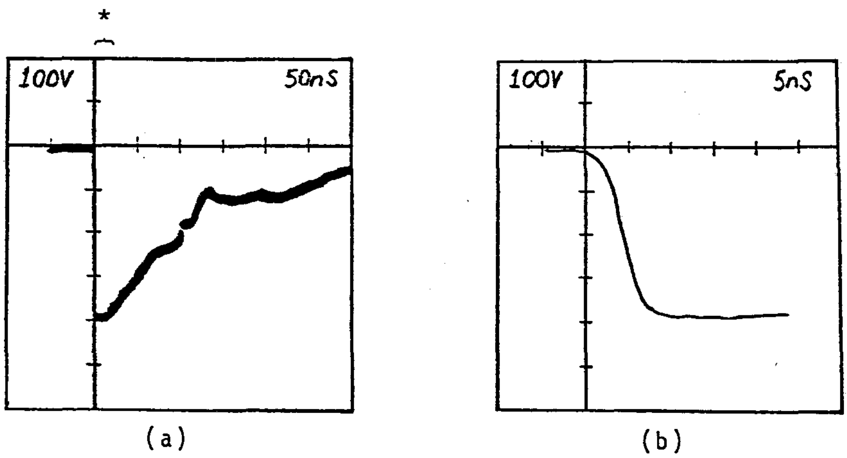

Fig. 3 Response of the Si Optoelectronic Switch with the Gap Width 0.8mm and Incident Energy of the Laser on the Gap of Approximately 20 μJ. Fig. 3 (b) is the Ten Times Magnified Version of the Part Marked * in Fig. 3 (a). A Bias is the Pulsed Bias of -640 V.

2.3 Analytical

In this section, calculated characteristics of the device in Fig. 1 are described. A trigger by a picosecond optical pulse to the Si OE switch at $t=0$ produces a step-wise optical pulse $P_{in}(t)$. Suppose $P_{in}(t)$ is represented by the waveform in Fig. 4. In Fig. 4, t_r denotes the rise-time of MOD.1. The transmitted optical power $P_t(t)$ is given by the following set of the three equations:

$$P_t(t) = \frac{1}{4} P_{in}(t) \; [\, 1 + \cos(\pi(\alpha + V(t)/V_\pi))\,] \tag{3}$$

$$V(t) = Z_0 G(t) V_B / (1 + 2Z_0 G(t)) \tag{3'}$$

$$G(t) = \frac{e\eta}{h\nu} (\mu_e + \mu_h) \frac{1}{r^2} \int_0^t P_t(t-T) e^{-(t-\tau)/\tau_0} d\tau \tag{3''}$$

where α is a bias retardation factor, V_π , a half-wave voltage, V_B , a bias voltage, Z_0 , a characteristic impedance of the transmission line (50 ohms), $G(t)$, a conductance across the gap of the GaAs OE switch, $\mu_e + \mu_h$, a sum of electron and hole mobilities in GaAs (≃10000 $cm^2/V\cdot s$), r , a gap width, and τ_0, a carrier lifetime in GaAs (≃ 100ps). Equation (3) is evaluated in Fig. 5 with r = 10 μm and wavelength of optical source 0.5 μm.

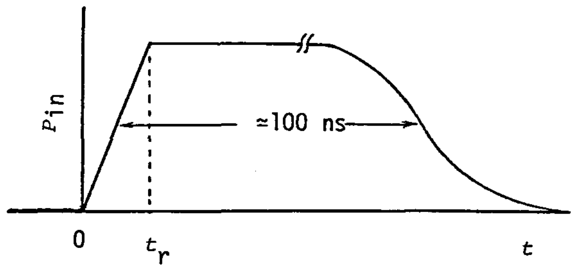

Fig. 4 Supposed Waveform of the Incident Pulse $P_{in}(t)$.

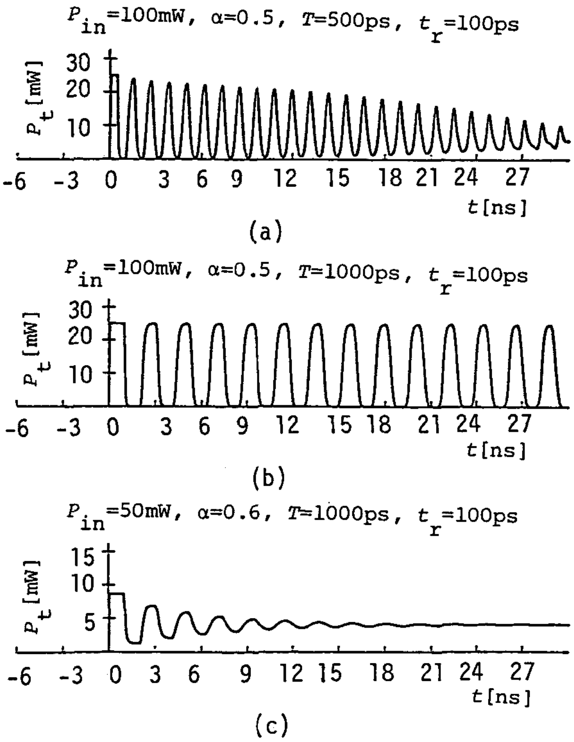

Fig. 5 Calculated Characteristics of the Optical-Waveform Synthesizer.

In Fig. 5, as parameter, we take the pulse height of the incident power P_{in}, the optical bias retardation factor α, the delay time of the optical fiber T, and the rise-time of the MOD.1, or t_r.

3. OPTICAL-PULSE SHAPING

3.1 Experimental Setup

Figure 6 shows the experimental setup for optical-pulse shaping whose configuration is the same as that of the device in Fig. 1. However, only Si OE switches are involved in Fig. 6. Figure 6 also includes an optical-pulse-waveform monitor composed of the same elements as those in the pulse shaper (principle of the monitor is described in Section 3.2). The more specific configuration of the optical-pulse shaper is given in Fig. 7. A half-wave voltage of the modulator in the pulse shaper is about 200 V for wavelength λ of 0.46 μ m. Electrooptic modulators used are Pockels' cells consisting of $LiTaO_3$, controlled by the Si OE switch. As a light source, we employed a dye laser pumped by the N_2 laser. Take $P_{in}(t)$ as a laser pulse from the dye laser. The beamsplitter devides $P_{in}(t)$ into the incident pulse $P_{inc.}(t)$ on the pulse shaper and the trigger pulse $P_{trig.}(t)$ to the waveform monitor. The delayed trans-mitted pulse $P_{tran.}(t-T)$ turns on the Si OE switch I, that causes the opaque state in the modulator, and since the carrier lifetime is much longer than the pulse width involved here (width of the pulse from the dye laser $\simeq$3 ns << 100 ns), the "on" state of the Si OE switch continues long after $P_{inc.}(t)$ goes through the modulator. Hence, the incident optical pulse $P_{inc.}(t)$ is shaped into the pulse $P_{tran.}(t)$ with the pulse width of approximately T. The use of a GaAs OE switch instead of the Si one can make a pulse train with the width T for each pulse because of the much shorter carrier lifetime.

3.2 Principle of Waveform Monitoring

The shaped optical pulse $P_{tran.}(t)$ has the pulse duration on the order of subnanosecond. Hence, special equipment is required to monitor the waveform of $P_{tran.}(t)$. We constructed the monitoring system comprising of the $LiTaO_3$ Pockels' cell and the Si OE switch. In this section, the principle of the monitor is given. The pulse $P_{trig.}(t)$, after going through the optical delay τ, triggers the Si OE switch, that gives the gated pulse $P_{tran.}(t)U(t-\tau)$ as the output pulse $P_{out}(t,\tau)$, where $U(t)$ is the unit step function. Changing the value of τ from τ_0 to $\tau_0+(N-1)\Delta\tau$ by the increment of $\Delta\tau$ gives a train of N-pulses $P_{out}(t,\tau_0+i\Delta\tau)$, ($i$ =0,1....,N-1). The pulses $P_{out}(t,\tau_0+i\Delta\tau)$ are converted into electric signals and integrated to become V_i which is proportional to energy of $P_{out}(t,\tau_0+i\Delta\tau)$, or

$$V_i = V(\tau_0+i\Delta\tau) \propto \int_{-\infty}^{\infty} P_{tran.}(t-\tau_0)U(t-\tau_0-i\Delta\tau)\,dt \tag{4}$$

In Fig. 8, oblique-lined areas correspond to V_i. Cross-oblique-lined areas correspond to $V_i - V_{i+1}$. Hence, $(V_i - V_{i+1})/\Delta\tau$ is approximately proportional to the sampled value of $P_{tran.}(t-\tau_0)$ at $t=\tau_0+(i+1/2)\Delta\tau$ if the condition

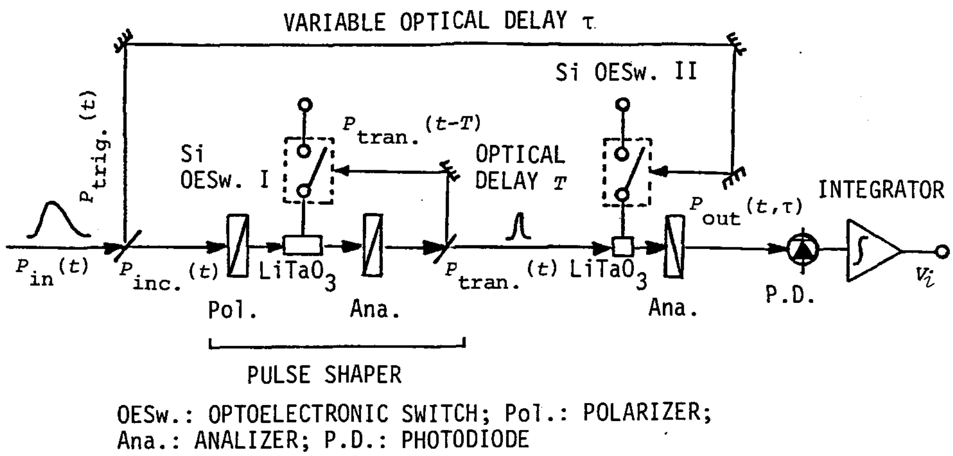

Fig. 6 Configuration of the Experimental Setup.

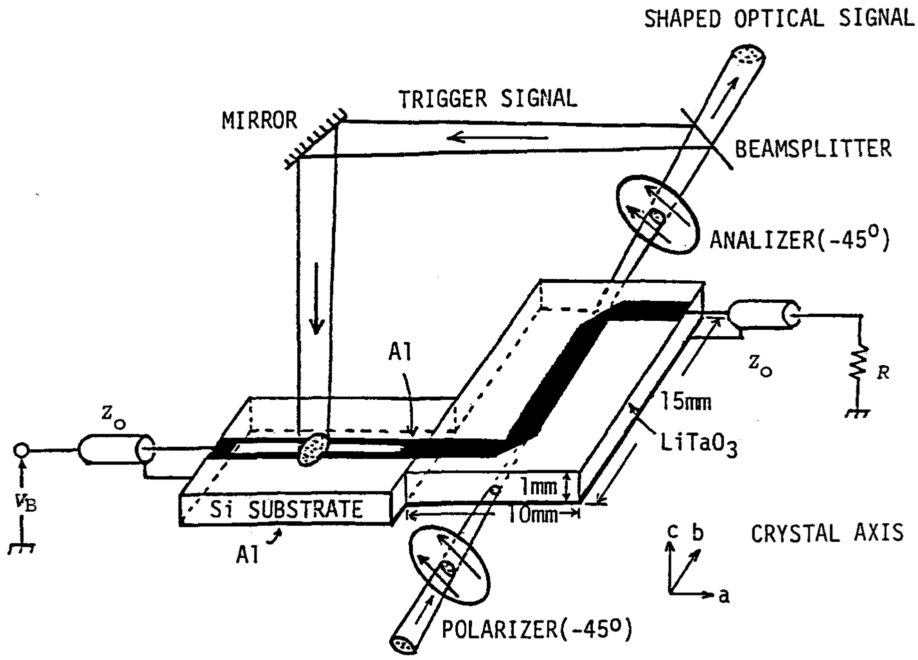

Fig. 7 Detailed Illustration of the Pulse shaper.

$$\left.\frac{dP_{tran.}(t-\tau_0)}{dt}\right|_{t=\tau_0+(i+1/2)\Delta\tau} \simeq \frac{P_{tran.}((i+1)\Delta\tau) - P_{tran.}(i\Delta\tau)}{\Delta\tau} \tag{5}$$

holds where $i = 0,1,2,....,N-2$.

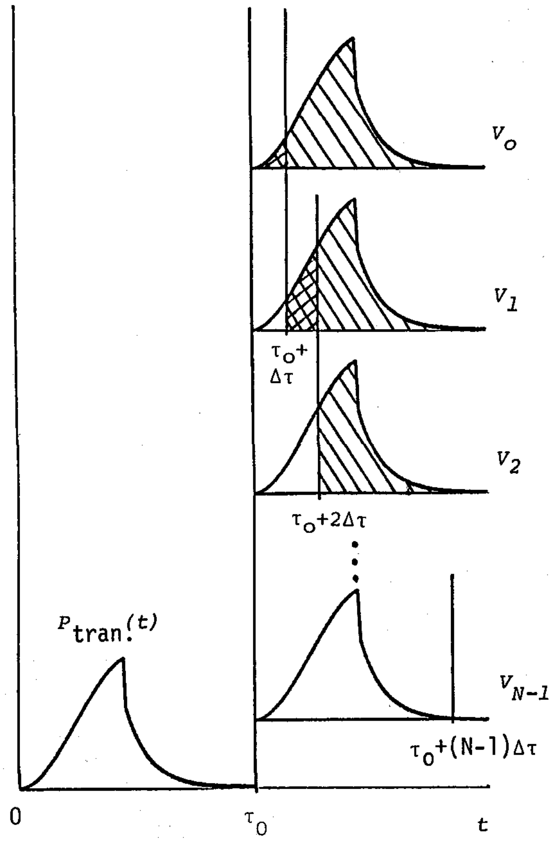

Fig. 8 Principle of Waveform Monitoring.

3.3 Experimental Results

Figure 9 indicates the experimental results: (a) and (b) are the sampled waveform of the shaped optical pulse $P_{tran.}(t)$;(a)' and (b)' are that of pre-shaped optical pulse $P_{inc.}(t)$. In Fig. 9 (a), the optical delay time T is taken as about 930 ps, and in Fig. 9 (b), $T \simeq 600$ ps.The time resolution in the pulse monitoring, or $\Delta\tau$, is 330 ps. The Si OE switch I is off when $t < T$,and at $t=T$,the OE switch turns on. The "on" state continues for about 100 ns on account of the 100-ns-carrier-lifetime in Si. Since the width of the optical pulse involved here is approximately 3 ns, the Pockels' cell controlled by the Si OE switch works as a linear optical gate. In Fig. 9 (a) and (a)', the Si OE switch I turns on at a time when the majority of energy of $P_{inc.}(t)$ passes through the pulse shaper. Hence, it is difficult to see whether $P_{inc.}(t)$ is shaped or not. In Fig. 9 (b) and (b)', however, the incident optical pulse $P_{inc.}(t)$ has enough power before and after the turn-on time of the Si OE switch I, or T : it is clear that the optical pulse shaper works.

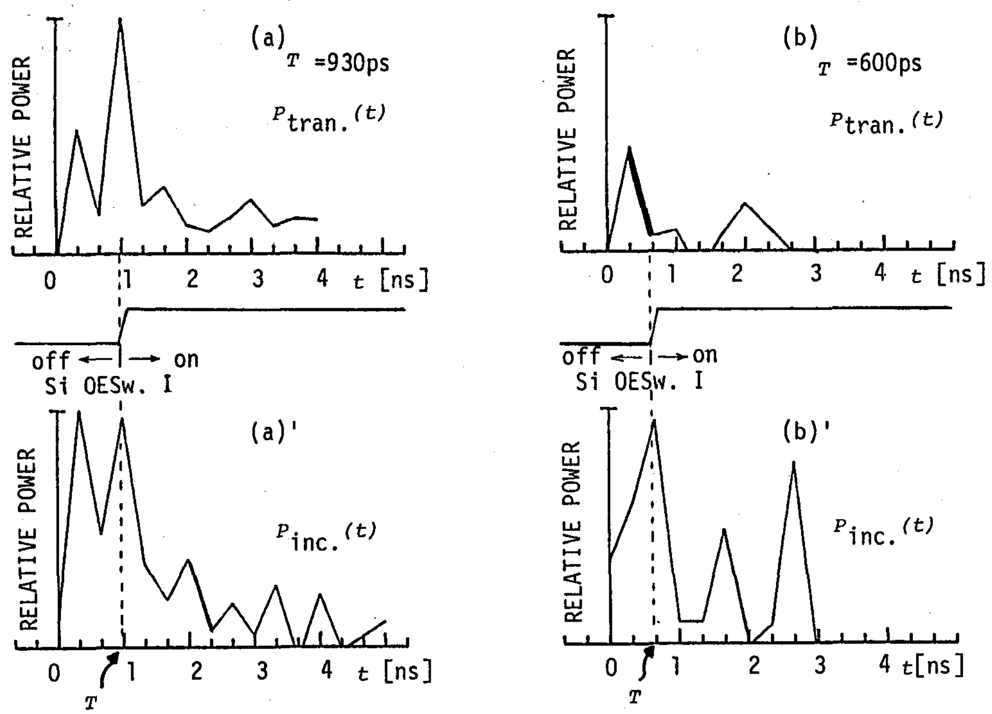

Fig. 9 Experimental Results.

3.4 Discussion

In Fig. 3, the response of the Si OE switch measured by an oscilloscope (100 MHz) is given. Since the rise-time of the switch is limited by the bandwidth of the oscilloscope, nothing definite about the rise-time is known from Fig. 3. In this section, the rise-time of the switch is estimated from the results of Section 3.3. In Fig. 9 (b), the negative-slope portion with heavy solid line is determined by the rising characteristic of the Pockels' cell in the pulse shaper which is controlled by the Si OE switch I. Therefore, the rising response of the Si OE switch I causes the negative slope in Fig. 9 (b). By measuring this negative slope, the rise-time of the switch can be evaluated. Given Fig. 9 (b), a fall-off time in the region with heavy solid line is 330 ps which is the time resolution of the monitor. Hence, the rise-time of the Si OE switch is, at least, estimated to be less than 330 ps.

4. CONCLUSIONS

We have described the optical waveform synthesizer with utilizing both GaAs- and Si-optoelectronic switches. The characteristic prospect of this device is faster operation. (From the numerical calculations, a train of pulses with a pulse width for each pulse on the order of subnanosecond can be obtained from this synthesizer.) As a preliminary experiment, optical-pulse shaping with Si OE switches was done, and the rise-time of the Si OE switches was evaluated to be less than 330 ps from the results in the case of illumination of a laser pulse from the dye laser on the gap of the switches. It is expected that the use of a small-gap-width-optoelectronic switch and low-half-wave-voltage modulator enables us to demonstrate the optical-waveform synthesizer with the use of a cw laser.

REFERENCES

(1)E. Garmire: Laser Focus, Vol. 18, No.1, (1982), 78.
(2)H. M. Gibbs *et al.* : Appl. Phys. Lett., Vol. 41, (1982), 221.
(3)R. Koga *et al.* : 1980 European Conference on Optical Systems and Applications, Proc. of the Society of Photo-Optical Instrumentation Engineers, Vol. 236, (1981), 373.
(4)C. H. Lee and V. K. Mathur: IEEE J. Quantum Electron., QE-17, (1981), 2098.
(5)D. H. Auston: Appl. Phys. Lett., Vol. 26, (1975), 101.
(6)J. Agostinelli *et al.* : Appl. Phys. Lett., Vol. 35, (1979), 731.